



# Nonlinear Dynamics of Vehicle Traction

B.J. OLSON<sup>1,2</sup>, S.W. SHAW<sup>2</sup> AND G. STÉPÁN<sup>3</sup>

## SUMMARY

The purpose of this study is to understand the nonlinear dynamics of longitudinal ground vehicle traction. Specifically, single-wheel models of rubber-tired automobiles under straight-ahead braking and acceleration conditions are investigated in detail. Customarily, the forward vehicle speed and the rotational rate of the tire/wheel are taken as dynamic states. This paper motivates an alternative formulation in which wheel slip, a dimensionless measure of the difference between the vehicle speed and the circumferential speed of the tire relative to the wheel center, replaces the angular velocity of the tire/wheel as a dynamic state. This formulation offers new insight into the dynamic behavior of vehicle traction. The unique features of the modeling approach allow one to capture the full range of dynamic responses of the single-wheel traction models in a relatively simple geometric manner. The models developed here may also be useful for developing and implementing anti-lock brake and traction control control schemes.

## 1. INTRODUCTION

In studies of vehicle traction the gross vehicle dynamics and tire/wheel dynamics can be captured by lumped mass models. Simplified models that are often considered for longitudinal braking and acceleration include the single-wheel model [1–3], and a two-dimensional, two-wheel model (front and rear) [1, 2], or full four-wheel models for cornering [1, 2]. The dynamics of these systems involve interactions between the vehicle, the tire/wheel assemblies, and the road surface. The force that ultimately slows or accelerates the vehicle is the longitudinal friction force between the road and tire, which can be empirically described in terms of a slip condition at the interface. Thus, writing the equations of motion for any rubber-tire vehicle system requires a description of the friction force generated at the tire/road interface, in addition to the usual laws of motion.

Experimental evidence shows that the longitudinal friction force is proportional to the normal force at the contact [1–3], with a coefficient of friction serving as the

<sup>1</sup>Address correspondence to: B.J. Olson, Department of Mechanical Engineering, Michigan State University, East Lansing, MI 48824, USA. E-mail: olsonbr1@egr.msu.edu

<sup>2</sup>Department of Mechanical Engineering, Michigan State University, East Lansing, MI 48824, USA.

<sup>3</sup>Department of Applied Mechanics, Budapest University of Technology and Economics, Budapest, Hungary.

'constant' of proportionality. This coefficient can be conveniently modeled in an empirical manner that depends on the slip [4, 5], which is a dimensionless measure of the difference between the vehicle speed and the circumferential speed of the tire relative to the wheel center. During braking (resp. acceleration), this difference is generated by a brake (resp. engine) torque on the wheel, which acts against (resp. with) the inertia of the vehicle. The slip depends on the dynamics of the vehicle and the tire/wheel, and it also influences their dynamics through the friction force. This 'feedback' results in a system of coupled equations of motion for the vehicle and the tire/wheel. These equations of motion are most often formulated in terms of the vehicle's speed relative to ground and the absolute rotational rate of the tire/wheel. This is a very natural formulation, wherein the slip is merely an internal variable defined in terms of the system's dynamic states, which is used to compute the friction force that appears in the equations of motion.

In this paper, a formulation is considered in which the slip is taken to be a dynamic state variable, replacing the absolute rotational rate of the tire/wheel. Liu and Sun [6] have developed the equations of motion for a quarter-car model in this way, but their investigation focuses on control algorithms based on gain-scheduling, rather than general dynamic behavior. The formulations herein focus not on control, but the general dynamic characteristics of vehicle traction. Only single-wheel braking and acceleration models are developed here; two-wheel models are considered in a companion paper [7]. It will be shown that the equations of motion take on forms that lend themselves to relatively simple investigation and interpretation using tools from nonlinear dynamics. Specifically, this formulation allows the dynamics for the entire range of vehicle speeds and slip values to be captured by a scalar function (one for each model) that is defined in terms of the slip, the brake or engine torque, and the friction/slip relationship. These functions describe completely the behavior of a given vehicle during braking (resp. acceleration) and under a constant or slowly varying brake (resp. engine) torque.

The dynamic models presented here are capable of describing both transient and steady tractive performance. Most importantly, they clearly demonstrate how a vehicle can undergo stable braking or acceleration and/or lockup, depending on the brake/engine torque, the friction characteristic, and the vehicle parameters. These models also allow one to clearly see how transitions between operating states occur as parameters and conditions are varied. In fact, a single set of phase plane diagrams, drawn at varying brake/engine torque levels, completely captures the entire range of possible behaviors for a given friction characteristic.

One of the more interesting findings of this study is a stability result related to brake lockup. The standard assumption is that the brake torque can increase until the slip reaches a value that corresponds to the maximum coefficient of friction, beyond which lockup occurs [1, 2]. Under steady-state braking conditions the corresponding maximum brake torque is typically assumed to be equal to the peak moment provided

by the friction force about the wheel center. In this work it is shown that this result is actually an approximation that is only accurate when the inertia of the tire/wheel is very small compared to that of the vehicle. Since this is generally the case, the approximation works well, but the present results determine where instability to lockup actually occurs, and also systematically shows how the approximation is obtained.

It is recognized that slip is notoriously difficult to measure in practice, primarily since it is not a simple matter to determine the vehicle speed relative to ground. (The speedometer uses the tire circumferential speed, which does not match the vehicle speed during slip – and this is precisely when both speeds are required to compute the slip [8]). However, since methods exist for estimating the slip [9–11], models such as those developed here may be useful for developing and implementing anti-lock brake systems (ABS) and traction control systems (TCS).

The paper is organized as follows. The single-wheel braking model is developed first in a systematic manner, thus laying the necessary groundwork for the development and analysis of a single-wheel acceleration model. The equations of motion are presented and the need to quantify the available friction force for braking is specified. This motivates an investigation of the tire/road interface and leads to the introduction of force coefficient characteristics as a function of longitudinal wheel slip. The equations of motion are hence cast into a framework that is convenient for a nonlinear dynamic analysis. Two formulations are considered: one in which the dynamic states are taken to be the forward vehicle speed and the angular speed of the tire/wheel, and one in which wheel slip replaces the angular speed as a dynamic state. The latter formulation is pursued in detail. Global features of the braking model are discussed, including steady-slip conditions, local stability of slip dynamics, hysteresis, and the transition to unstable braking (lockup). Finally, a single-wheel acceleration model is similarly developed and analyzed. The paper closes with some conclusions and directions for future work.

## 2. THE SINGLE-WHEEL BRAKING MODEL

A quarter-car model is developed in this section in order to illustrate the fundamental aspects of vehicle braking. This single-wheel model is unrealistic by virtue of its simplicity, and it clearly fails to capture some important dynamical features (e.g., dynamic load transfer). It nevertheless serves to facilitate an understanding of the basic dynamic characteristics of vehicle braking. In fact, the approach taken here lays the necessary groundwork for the formulation and analysis of two- and four-wheel models. Two-wheel traction models are considered in a companion paper.

As depicted in Figure 1, the quarter-car model consists of a single wheel constrained to move longitudinally in the  $x$ -direction at a speed  $u$  and with a rotational

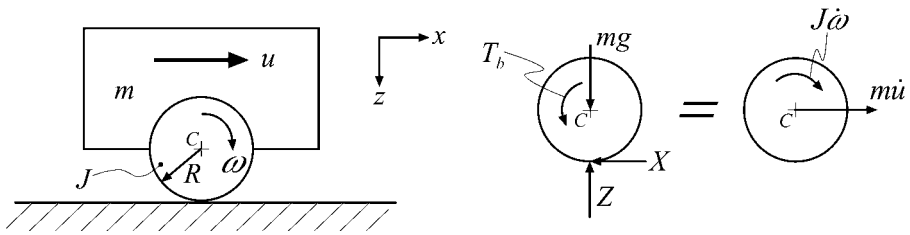


Fig. 1. Schematic of the single-wheel braking model and corresponding free body diagram.

rate  $\omega$ . Denoted by  $R$  and  $J$  are its effective rolling radius and polar moment of inertia, respectively. The effect of a braking mechanism on the vehicle wheel is captured by the brake torque  $T_b$ , which opposes the forward motion of the system. The vertical reaction force  $Z$  balances the static weight  $mg$ , while the longitudinal force  $X$  serves to slow the vehicle in braking. By summing forces in the  $x$ - and  $z$ -directions and moments about the mass center  $C$  of the vehicle/wheel, the system equations are found to be:

$$m\dot{u} = -X, \quad (1)$$

$$Z = mg, \quad (2)$$

$$J\dot{\omega} = RX - T_b, \quad (3)$$

where  $m$  is the mass of the vehicle-wheel combination and  $g$  is the acceleration due to gravity. Overdots denote differentiation with respect to time.

In general, there are a number of forces acting on a vehicle that may give rise to a deceleration. The model considered here includes only the longitudinal brake force  $X$ , which is discussed in detail in the next section. Other sources of deceleration in braking include driveline drag, grade, rolling resistance, and aerodynamic drag.

## 2.1. Tractive Properties

The primary force of interest in studies of vehicle traction is the longitudinal force  $X$ , which acts on the vehicle through a tire/road contact patch. Experimental evidence shows that this friction force is proportional to the normal force  $Z$  at the contact and is a consequence of the relative difference between the vehicle speed  $u$  and the rolling speed of the tire  $\omega R$ . The ‘constant’ of proportionality is responsible for the friction coupling, and can be empirically determined by a friction characteristic in terms of road test data and wheel slip, which is a dimensionless measure of the difference between  $u$  and  $\omega R$ . Since the friction characteristic captures the typifying quantities of

a particular tire/road combination – including slip stiffness at zero slip and peak brake force values – it can be regarded as a tire model that characterizes the tire behavior on a given road surface. The tractive properties are now discussed in terms of wheel slip, the tire/road interface and attendant friction law, and a tire model.

### 2.1.1. Wheel Slip

The longitudinal friction force  $X$  is a consequence of the relative difference between the vehicle speed  $u$  and the rolling speed of the tire, which is given by  $\omega R$ . Wheel slip is defined in terms of this difference as<sup>1</sup>

$$s \equiv \frac{u - \omega R}{\max(u, \omega R)}. \quad (4)$$

It is assumed and taken as convention that  $u > 0$  and  $0 \leq \omega R \leq u$  in vehicle braking. Thus,  $s = \frac{u - \omega R}{u}$  is defined on the unit interval  $I = [0, 1]$ , taking on the limiting values of  $s = 0$  for free rolling ( $u = \omega R$ ) and  $s = 1$  for wheel lockup ( $\omega R = 0$ ). The former case  $u = \omega R$  implies the absence of a brake torque. The definition of slip, along with the convention that  $\omega R \leq u$  allows for two possibilities for steady-state vehicle braking with nonzero initial speed: (1) finite rotation of the wheel while the vehicle decelerates; and (2) deceleration under lockup conditions. It is noted that the case of lockup is undesirable since steerability, directional stability, and general control over a vehicle is severely degraded in such a state [1, 2].

### 2.1.2. The Tire/Road Interface and Friction Law

In a rubber tire, wheel slip results in the deformation and sliding of tread elements in the tire/road contact patch, which in turn sustains the friction force  $X$  in braking. Indeed, it is through this important interface between the road surface and tire tread that braking is negotiated. In general, the microscopic physical description of the said phenomenon is complicated and involves more physics than what are needed here. (See, for instance, [1, 2].) It suffices to capture these interactions by the simple algebraic relationship:

$$X = \mu(s)Z, \quad (5)$$

which is known as *the friction law* or *creep force equation*. The longitudinal force coefficient  $\mu : I \rightarrow I$  is experimentally determined in terms of road test data and is the subject of the next section.

<sup>1</sup>The maximum function  $\max(u, \omega R)$  allows the use of Equation (4) to define longitudinal wheel slip for both vehicle braking and acceleration. In braking  $u < \omega R$ , while  $u > \omega R$  for vehicle acceleration.

### 2.1.3. Friction Characteristic and Tire Model

The friction coupling between a rubber tire and road surface depends on a number of physical parameters involving tire construction, inflation and wear, the tire/road interface, and vehicle speed and loading [1–3]. Since a general theory that can accurately predict the longitudinal brake force in terms of wheel slip has yet to be developed, friction coupling is necessarily determined experimentally. Various methods exist to relate the brake and normal forces  $X$  and  $Z$  in terms of a friction characteristic  $\mu(s)$ . See, for example, [9, 10]. The resulting data can then be represented by a formula.

Figure 2 shows graphical representations of some typical longitudinal friction characteristics. The initial rate at which  $\mu(s)$  increases with increasing slip is dependent on the properties of the tire. For wet and dry asphalt the characteristics increase until a peak value  $\mu_p = \mu(s_p)$  is attained. This typically occurs between 10 and 20% slip, yielding maximum braking forces of 25–50% and 70–90% of the vertical load for wet and dry asphalt, respectively. The friction characteristics then exhibit a gradual decrease to  $s = 1$  (wheel lockup). For gravel and packed snow, the behavior of the friction coefficient characteristics are qualitatively different. Peak values occur at wheel lockup (here,  $s = s_p = 1$ ) and are the consequence of plowing conditions on the deformable surfaces. Ice characteristics (not shown) are similar to those for wet and dry asphalt, differing mostly in the resulting peak values [1–3].

An analytical treatment of these friction characteristics is possible by employing the widely used Pacejka tire model [4, 5]. It is described by the so-called *Magic Formula* which is given by:

$$y(x) = D \sin(C \arctan(Bx - E(Bx - \arctan(Bx))))), \quad (6)$$

where the parameters  $B$ ,  $C$ ,  $D$ , and  $E$  are the *stiffness*, *shape*, *peak*, and *curvature* factors. See [4] for typical values of these coefficients. Horizontal and vertical shifts

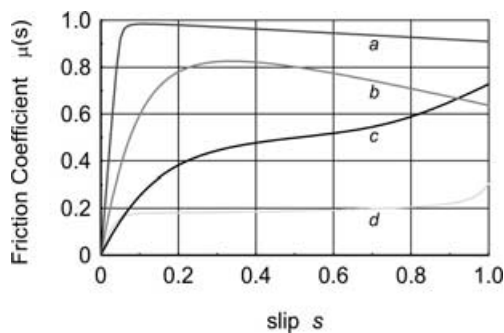


Fig. 2. Typical longitudinal friction characteristics: (a) dry asphalt; (b) wet asphalt; (c) gravel; and (d) packed snow.

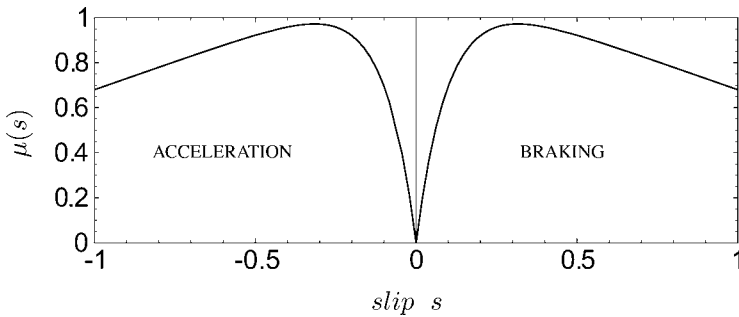


Fig. 3. Friction characteristics employed in numerical simulations.

of a characteristic are attained by the transformations:

$$Y(\chi) = y(x) + S_v, \quad x = \chi + S_h,$$

where  $S_v$  is the vertical shift and  $S_h$  is the horizontal shift. The function  $Y(\chi)$  can represent all steady-state tire characteristics – including the brake force  $X$ , side force, and self-aligning torque – in a physically meaningful and straightforward way. The variable  $\chi$  denotes either slip angle (the angle subtended from the direction of wheel travel to the direction of wheel heading) or longitudinal wheel slip  $s$ . In light of Equations (2) and (5), note that the Magic Formula can be scaled to represent  $\mu(s)$  directly on  $I$ .

For the purpose of more efficient numerical simulations, a simple friction characteristic was devised for the present study and is given by:

$$\mu(s) = c_1(1 - e^{-c_2s}) - c_3s, \quad s \in I. \quad (7)$$

This function is unimodal with a peak value of  $\mu_p = 0.972$  at  $s_p = 0.316$  and hence behaves similarly to wet and dry asphalt characteristics. Equation (7), which is shown in Figure 3 for  $c_1 = 1.18$ ,  $c_2 = 10.0$ , and  $c_3 = 0.5$ , was employed for all calculations and numerical simulations involving  $\mu(s)$  for the vehicle braking model. The characteristic shown for  $s \in [-1, 0]$  is employed for vehicle acceleration in Section 3.

## 2.2. Equations of Motion

During wheel slip, the single-wheel model possesses two dynamic states and hence requires a set of two coordinates to describe its motion. By inspection of Equations (1)–(5), it is clear that two of three possible variables of interest could be chosen as the independent variables, namely,  $u$ ,  $\omega$ , or  $s$ . The equations of motion for the single-wheel braking model are developed first in terms of  $u$  and  $\omega$  as dynamic states, and the qualitative dynamics are captured in the  $(u, \omega R)$  phase plane. Though such a description

is physically illuminating, it is subsequently shown in Section 2.2 that a formulation of the equations of motion in terms of  $u$  and  $s$  as dynamics states lends itself to a relatively simple interpretation. Specifically, it will be shown that the latter formulation allows the dynamics for the entire range of vehicle speeds and slip values to be captured by a single function that is defined in terms of wheel slip and the brake torque.

2.2.1.  $u$  and  $\omega$  as Dynamic States

The common formulation of the equations of motion makes use of the speed  $u$  of the vehicle relative to ground and the absolute rotational rate  $\omega$  of the tire/wheel as dynamic states. Then the system dynamic equations are:

$$\left. \begin{aligned} \dot{u} &= -\mu(u, \omega)g \\ \dot{\omega}R &= gH(u, \omega) \end{aligned} \right\}, \quad 0 \leq \omega R \leq u, \tag{8}$$

where wheel slip is merely an internal variable. The restriction  $0 \leq \omega R \leq u$  ensures that  $s \in I$ , according to the convention of wheel slip in braking. The function:

$$H(u, \omega) = \nu\mu(u, \omega) - \Upsilon_b \tag{9}$$

is dimensionless, where  $\nu = \frac{mR^2}{J}$  is the dimensionless ratio of vehicle to wheel inertia (typically  $\nu \gg 1$ ), and  $\Upsilon_b = \frac{K}{Jg}T_b$  is the dimensionless brake torque.

2.2.2. The  $(u, \omega R)$  Phase Plane

Figure 4a shows trajectories in the  $(u, \omega R)$  state space for  $\nu = 15$  and  $\Upsilon_b = 12$ . The rolling speed  $\omega R$  of the tire is defined along the ordinate while the vehicle speed  $u$  is

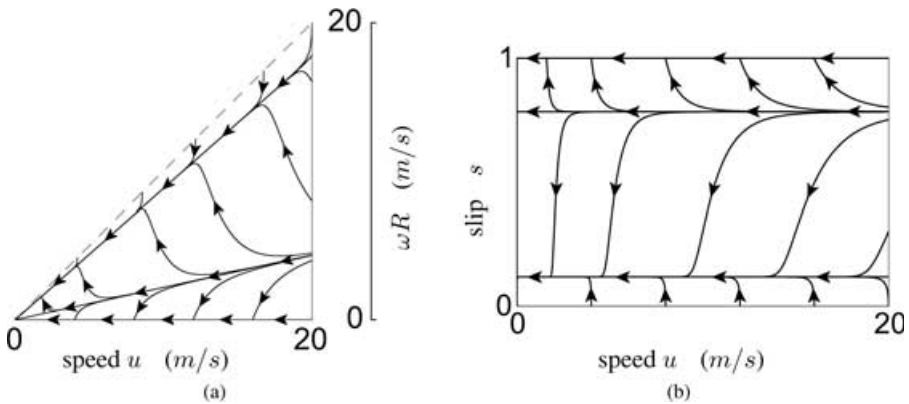


Fig. 4. State space descriptions for the single-wheel braking model for  $\nu = 15$  and  $\Upsilon_b = 12$ : (a) in  $u$  and  $\omega R$ ; (b) in  $u$  and  $s$ .

defined along the abscissa. Wheel slip is implicitly defined in terms of these states by:

$$\omega R = (1 - s)u, \quad (10)$$

which follows from the definition given by Equation (4). Equation (10) shows that radial lines originating from  $(u, \omega R) = (0, 0)$  are lines of constant slip for which there is a linear relationship between  $u$  and  $\omega R$ . Since  $s$  is defined on the unit interval for vehicle braking, the dynamics need only be considered in the region:

$$\mathcal{F} = \{(u, \omega R) | u \geq 0, 0 \leq \omega R \leq u\}. \quad (11)$$

Thus, trajectories are bounded by the line  $\omega R = u$ , which corresponds to  $s = 0$  (free rolling), and the line  $\omega R = 0$ , or the  $u$ -axis, which corresponds to  $s = 1$  (wheel lockup). For a particular brake torque, certain constant-slip radial lines are invariant under the dynamics. The corresponding constant slip values shall be denoted by  $s^*$ . Any such set that satisfies these conditions and the equations of motion define invariant linear manifolds in the  $(u, \omega R)$  phase plane, which are denoted by:

$$\mathcal{W}_b^* = \{(u, \omega R) | \omega R = (1 - s^*)u, s^* \in I\}. \quad (12)$$

Under certain conditions (to be determined subsequently), the  $u$  axis is also an invariant manifold (where  $s = 1$ ) and is denoted by:

$$\mathcal{W}_b^L = \{(u, \omega R) | u \geq 0, \omega R = 0\}, \quad (13)$$

where the superscript  $L$  indicates lockup. There are, for example, three such invariant manifolds when  $\Upsilon_b = 12$  (see Fig. 4a) with one corresponding to lockup conditions, that is,  $\mathcal{W}_b^L$ . All trajectories started in  $\mathcal{F}$  rapidly approach either  $\mathcal{W}_b^*$  or  $\mathcal{W}_b^L$  as  $u$  decreases (since  $\dot{u} < 0$ ) and evolve essentially along the invariant manifold toward zero speed at  $(u, \omega R) = (0, 0)$ . Trajectories started on, or that approach  $\mathcal{W}_b^*$ , represent stable braking, while trajectories that approach  $\mathcal{W}_b^L$  correspond to unstable braking, or lockup conditions. These invariant manifolds, if they exist, serve two purposes: they (1) define steady-slip conditions that are invariant under the dynamics and under which the vehicle decelerates to zero speed; and (2) separate regions of stable and unstable braking. It would be desirable to quantify these manifolds without having to perform numerical simulations for several initial conditions.

In what follows, an alternative formulation is considered where wheel slip  $s$  replaces  $\omega R$  as a dynamic state. Figure 4 compares the state space description of the single-wheel braking model in the  $(u, \omega R)$  phase plane to its description in the  $(u, s)$  phase plane for  $\nu = 15$  and  $\Upsilon_b = 12$ . The alternative formulation yields a state space where, essentially, the point  $(u, \omega R) = (0, 0)$  is expanded to represent wheel slip on the unit interval at  $u = 0$ . In doing so, a singularity is introduced at  $u = 0$ ; but, as indicated in Figure 4b, the invariant manifolds  $\mathcal{W}_b^*$  and  $\mathcal{W}_b^L$  are easily identified in the  $(u, s)$  phase space as lines of constant  $s$ . It will be shown that a formulation of the equations

of motion in terms of  $u$  and  $s$  allows for the invariant manifolds, and hence steady-slip conditions and various operating regimes, to be captured by a single function that is defined in terms of wheel slip and the brake torque.

### 2.2.3. $u$ and $s$ as Dynamic States

Although it is very natural to cast the equations of motion in terms of the forward vehicle speed  $u$  and the tire/wheel rate of rotation, it is instructive to replace  $\omega$  with wheel slip as a state variable. Liu and Sun [6] have developed the equations of motion for a quarter-car model using  $u$  and  $s$  as dynamic states, but their investigation focuses on control algorithms based on gain-scheduling. Here the equations of motion are developed similarly but with emphasis on a form suitable for a nonlinear dynamic analysis. Evaluating the time rate of change of wheel slip (for  $\omega R \leq u$ ):

$$\dot{s} = \frac{R}{u^2}(\omega\dot{u} - u\dot{\omega}),$$

and performing the appropriate substitutions, the equations of motion may be cast in terms of  $u$  and  $s$ . The result is:

$$\left. \begin{aligned} \dot{u} &= -\mu(s)g \\ \dot{s} &= \frac{g}{u}h_b(s) \end{aligned} \right\}, \quad u > 0, \quad s \in I. \quad (14)$$

Since  $u > 0$  by convention,  $g > 0$ , and  $\mu(s) \in I$ , it follows that  $\dot{u} < 0$ , which is expected. The function:

$$h_b(s) = (s - 1 - \nu)\mu(s) + \Upsilon_b \quad (15)$$

is nondimensional, where, recall,  $\nu = \frac{mR^2}{J}$  is the ratio of vehicle inertia to wheel inertia and  $\Upsilon_b = \frac{R}{Jg}T_b$  is the dimensionless brake torque. Note that the brake torque term is additive, so that as  $\Upsilon_b$  is varied, the shape of  $h_b(s)$  does not change. It simply shifts up and down. Also, since typically  $\nu \gg 1$  (discussed subsequently), the shape of  $h_b(s)$  is close to that of  $-\nu\mu(s)$ .

The general features of the quarter-car model are best demonstrated by treating Equation (14) as a state-space representation of the single-wheel system and exploring its behavior in the  $(u, s)$  state space. It will be shown that this interpretation of the single-wheel model yields good insight into its dynamic response during transient and steady-state braking. The analysis begins by determining the steady-slip conditions and their local stability characteristics. A more detailed mathematical analysis follows in a discussion of the global features of the single-wheel braking model.

## 2.3. Steady-Slip Conditions

Equation (14) shows that, for nonzero  $u$  and a slip value  $s^*$  for which  $h_b(s^*) = 0$ , the time rate of change of slip is identically equal to zero. Correspondingly, wheel slip

remains constant at  $s = s^*$ , independent of the vehicle speed. This in turn ensures that the vehicle acceleration  $\dot{u} = -\mu(s^*)g$  is negative and constant. Here,  $\mu(s^*)$  is the longitudinal force coefficient corresponding to the fixed slip value. Under these conditions the vehicle speed monotonically decreases to zero according to the equation:

$$u(t) = u_o - \mu(s^*)gt, \quad u > 0, \quad 0 \leq t \leq t_f, \tag{16}$$

where  $u_o > 0$  is the initial speed at the instant when  $s = s^*$ , that is, when  $t = 0$ , and  $t_f$  corresponds to the time when  $u = 0$ . Wheel lockup also yields steady-slip conditions when  $s = 1$ . Under lockup conditions, the dynamics of the vehicle are described by Equation (16), with the coefficient of sliding friction  $\mu_L = \mu(s = 1)$  replacing  $\mu(s^*)$ .

### 2.4. Local Stability of Slip Dynamics

Before specifying a quantitative measure of stability, it is convenient to outline and adopt specific notation. First, recall that constant slip values  $s^*$  denote invariant points in the slip dynamics. They may be obtained by finding the zeros of  $h_b(s)$ , that is, by finding the roots of  $h_b(s^*) = 0$ . More precisely, the steady-slip values  $s^*$ , if they exist, define *invariant sets* of the system, since once  $s = s^*$  is attained,  $s$  remains at that value for all time, independent of the values of  $u$  (for  $u > 0$ ). Any such value of  $s = s^*$  may be either stable or unstable and shall be denoted by  $s^+$  and  $s^-$ , respectively. Local stability criteria of wheel slip follows from considering a small perturbation  $\eta(t) = s(t) - s^*$  away from one of these roots. Differentiating with respect to time, invoking Equation (14), and employing  $h_b(s^*) = 0$ , the local slip dynamics near  $s^*$  can be approximated to leading order by the linearized equation:

$$\dot{\eta} = \frac{g}{u} h'_b(s^*) \eta, \tag{17}$$

where  $(\cdot)' = \frac{d(\cdot)}{ds}$  denotes differentiation with respect to  $s$ . Since  $\frac{g}{u} > 0$ , Equation (17) shows that the perturbation grows exponentially fast when  $h'_b(s^*) > 0$  and decays exponentially when  $h'_b(s^*) < 0$ . Thus, the stability of the slip dynamics near  $s = s^*$  are determined by the slope of  $h_b(s)$  at  $s = s^*$ :

$$h'_b(s^*) = \mu'(s^*)(s^* - 1 - \nu) + \mu(s^*). \tag{18}$$

Stable and unstable steady-slip values are defined to be:

$$s^\pm = \{s | h_b(s^\pm) = 0, h'_b(s^\pm) \gtrless 0\}. \tag{19}$$

The corresponding stable and unstable invariant manifolds of the system in the  $(u, s)$  plane are defined by:

$$\mathcal{W}_b^\pm = \{(u, s) | u > 0, s = s^\pm\}. \tag{20}$$

For lockup there is a stable manifold:

$$\mathcal{W}_b^L = \{(u, s) | u > 0, s = 1\},$$

defined for parameter conditions under which  $h_b(1) \geq 0$ . The notation  $\mathcal{W}_b^*$  shall refer to either of the invariant manifolds  $\mathcal{W}_b^+$  or  $\mathcal{W}_b^-$  ( $\mathcal{W}_b^L$  not included).

### 2.5. Global Features of the Single-Wheel Braking Model

Equations (17) and (19) hint at the importance of  $h_b(s)$ , since steady-slip conditions and the local stability of the slip dynamics are completely determined in terms of this dimensionless function. In fact, the entire range of vehicle speeds and slip values are captured by  $h_b(s)$  under a constant brake torque or slowly varying brake torque. This is shown in Figure 5, where the function  $h_b(s)$  versus slip and the corresponding state space dynamics in  $u$  and  $s$  are depicted for  $\nu = 15$  and for various values of the nondimensional brake torque. The intersection of the function  $h_b(s)$  with the line  $h_b = 0$  defines the invariant points  $s^*$  [see Equation (19) and Table 1], and hence the invariant manifolds  $\mathcal{W}_b^*$  in the  $(u, s)$  space, which are defined by Equation (20).

For  $\Upsilon_b = 7$ , a small brake torque, only one invariant point exists, which is shown in Figure 5a as  $s^+$ . Since  $h'_b(s^*) < 0$  the steady-slip value  $s^+$  is stable and hence defines the invariant manifold  $\mathcal{W}_b^+$ . All initial conditions  $(u, s) = \{(u, s) | u > 0, s \in I\}$  result in stable braking at this parameter value, hence it is *globally stable*. This can be seen by noting that for  $s \leq s^*$ ,  $\dot{s} = \frac{g}{u} h_b(s) > 0$  so that  $s$  increases while for  $s > s^*$ ,  $\dot{s} = \frac{g}{u} h_b(s) < 0$  and hence  $s$  is decreasing. Therefore all initial conditions lead towards  $s = s^+$ .

By increasing the brake torque such that  $h_b(1) = 0$ , another fixed point is introduced at  $s = 1$  for which the slope of  $h'_b(s^*)$  is negative; hence it is unstable. It is denoted by  $s = s^-$  and defines the unstable invariant manifold  $\mathcal{W}_b^-$  in the  $(u, s)$  space. Note that the creation of the unstable invariant point  $s^-$  corresponds to the introduction of lockup at  $s = 1$ , which defines  $\mathcal{W}_b^L$ . This is essentially a saddle-node bifurcation creating the steady-slip values  $s^-$  and  $s = 1$ . Figure 5b shows this situation, where  $\mathcal{W}_b^-$  and  $\mathcal{W}_b^L$  are coincident at the brake torque level  $\Upsilon_b^L = 10.199$ . All trajectories lying below  $\mathcal{W}_b^- = \mathcal{W}_b^L$ , that is, in  $\{(u, s) | u > 0, s \in [0, 1)\}$ , are attracted to the invariant manifold  $\mathcal{W}_b^+$  and result in stable braking conditions. At this specific parameter value lockup ( $s = 1$ ) is unstable.

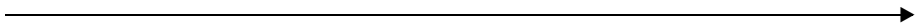


Fig. 5.  $h_b(s)$  versus  $s$  and corresponding state space descriptions in  $u$  and  $s$  for  $\nu = 15$ : (a)  $\Upsilon_b = 7$ ; (b)  $\Upsilon_b = \Upsilon_b^L = 10.199$ ; (c)  $\Upsilon_b = 12$ ; (d)  $\Upsilon_b = \Upsilon_b^{cr} = 15.250$ ; (e)  $\Upsilon_b = 18$ . See Table 1 for steady slip values.

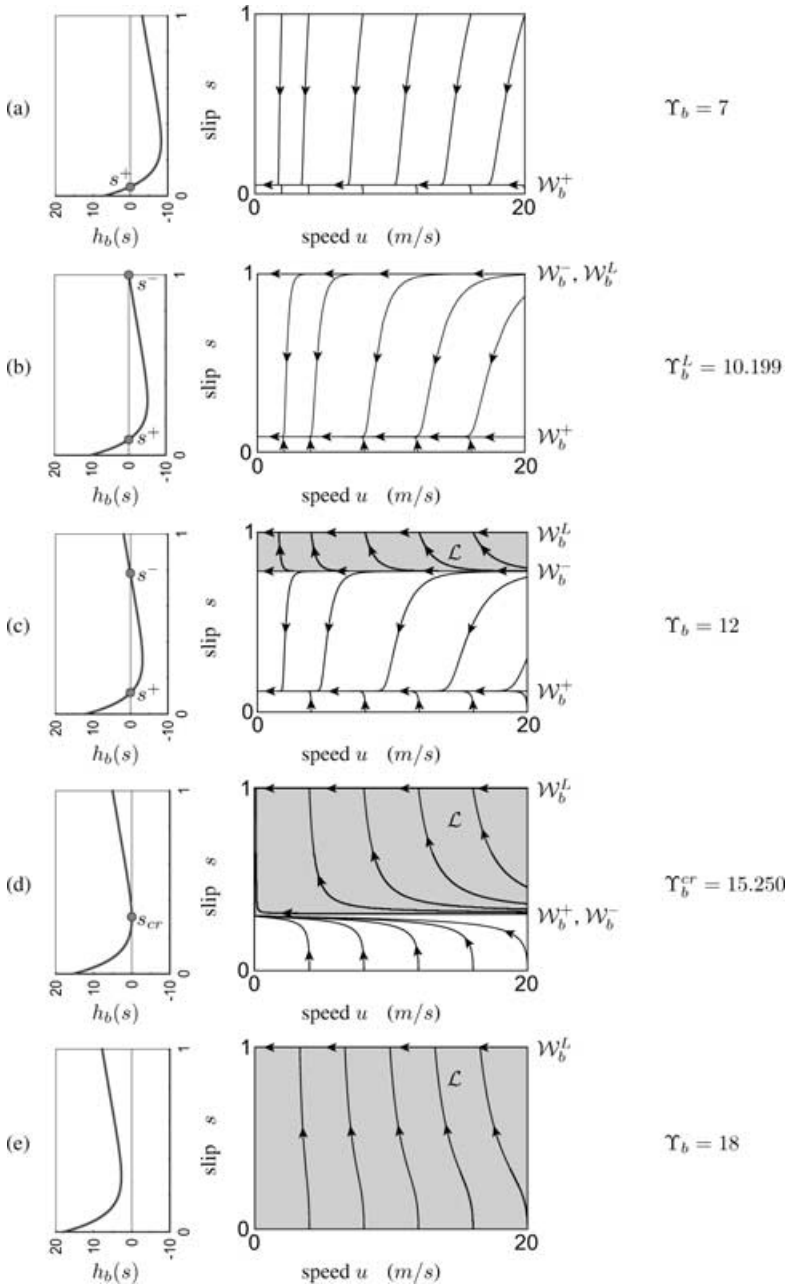


Table 1. Steady-slip values for the single-wheel braking model.

$\Upsilon_b$	$s^-$	$s_{cr}$	$s^+$
7	–	–	0.050
12	0.782	–	0.117
$\Upsilon_b^L = 10.199$	1	–	–
$\Upsilon_b^{cr} = 15.250$	–	0.304	–
18	–	–	–

As the brake torque is further increased (shown in Fig. 5c for  $\Upsilon_b = 12$ )  $s^-$  moves away from  $s = 1$ , which stabilizes  $\mathcal{W}_b^L$  and creates a lockup region. All trajectories above  $\mathcal{W}_b^-$ , that is, those with initial conditions in  $\{(u, s) | u > 0, s \in (s^-, 1]\}$ , tend to  $\mathcal{W}_b^L$  (indicating wheel lockup). Trajectories lying below  $\mathcal{W}_b^-$  are attracted to the invariant manifold  $\mathcal{W}_b^+$  and result in stable braking conditions.

Further increasing  $\Upsilon_b$  causes  $s^+$  and  $s^-$  to move toward each other. Eventually a critical brake torque  $\Upsilon_b^{cr} = 15.250$  is reached where the stable and unstable invariant points collide and mutually annihilate in a saddle node bifurcation at the critical slip value  $s = s_{cr} = 0.304$ . (See Fig. 5d.) For brake torques greater than  $\Upsilon_b^{cr}$  the invariant manifold  $\mathcal{W}_b^L$  is globally stable and wheel lockup occurs for all initial slip conditions. This situation is shown in Figure 5e where  $\Upsilon_b = 18$ .

The set of initial conditions for which a trajectory reaches the invariant manifold  $\mathcal{W}_b^L$  is called the *domain of attraction* of  $s = 1$  in the  $(u, s)$  state space and is denoted by:

$$\mathcal{L} = \{(u, s) | u > 0, s \in [s^-, 1]\}.$$

Trajectories started with initial conditions in  $\mathcal{L}$  (denoted by the shaded regions in Fig. 5) tend rapidly toward lockup at  $s = 1$ , subsequently move along  $\mathcal{W}_b^L$ , and monotonically approach the point  $(0, 1)$  according to Equation (16). This situation corresponds to braking under lockup conditions which, for wet and dry asphalt characteristics, is always non-optimum in terms of deceleration since  $\mu(s = 1) = \mu_L < \mu(s_p)$ . The domain of attraction of  $s^+$ , that is, the set of initial conditions for which a trajectory reaches the stable invariant manifold  $\mathcal{W}_b^+$ , is given by:

$$\mathcal{S} = \{(u, s) | u > 0, s \in I \setminus \mathcal{L}\}.$$

Trajectories started with initial conditions in  $\mathcal{S}$  rapidly converge toward the stable invariant manifold and evolve essentially along  $\mathcal{W}_b^+$ , according to Equation (16) toward the point  $(u, s) = (0, s^+)$ , where the vehicle has stopped. The rate at which the vehicle decelerates under steady-slip depends only on  $\mu(s^*)$ , that is, the particular friction characteristic and the value of  $s^*$ . Finally, trajectories started on the unstable invariant manifold remain on  $\mathcal{W}_b^-$  and monotonically evolve toward the point  $(0, s^-)$ .

This situation is physically unattainable, however, since any small perturbation in the system would cause a trajectory to leave  $\mathcal{W}_b^-$  and move into either  $\mathcal{S}$  or  $\mathcal{L}$ .

Note that, since  $\dot{s} \sim \frac{1}{u}$ , the rate at which a trajectory tends toward either  $\mathcal{W}_b^L$  or  $\mathcal{W}_b^+$  increases dramatically as  $u$  tends toward zero. In fact, from Equation (14), the time rate of change of wheel slip becomes infinite as  $u \rightarrow 0$  with  $s \neq 1, s^*$ . Hence, the vehicle must come to rest *under steady-slip conditions* for which  $s = 1$  or  $s = s^*$ . There are only two such physical possibilities: the vehicle decelerates to zero speed (1) at the rate  $\mu_L g$  with the wheels locked; or (2) with steady-slip at the absolute rate  $\mu(s^+)g$ . Peak steady-braking performance would entail steady slip at  $s = s_p$  for which the maximum deceleration is obtained and is equal in magnitude to  $\mu_p g$ . However, it will be shown in Section 2.7 that the transition to lockup occurs before  $s^*$  can reach  $s_p$ . Thus, since  $s_p$  cannot be reached under stable braking conditions, optimum braking would entail steady-slip at  $s = s_{cr}$ . The corresponding deceleration is equal in magnitude to  $\mu_{cr} g = \mu(s = s_{cr})g < \mu_p g$ . But since  $s_{cr}$  is a saddle node in the slip dynamics, any perturbation in the system could send the braking conditions into wheel lockup. The critical brake torque needed to sustain optimum braking, and the corresponding lockup instability at that brake torque value, are discussed in Section 2.7.

It is again stressed that the function  $h_b(s)$  completely determines the nonlinear dynamic behavior of the single-wheel system in braking over the entire range of vehicle speeds and slip values. Given the dimensionless brake torque  $\Upsilon_b$ , one need only calculate the zeros of  $h_b(s)$  to quantify steady-slip values and the corresponding invariant sets. The slope of  $h_b(s)$  at these steady-slip values indicates the stability of the corresponding invariant manifolds. With this knowledge, a complete state space description of the vehicle dynamics can be constructed for the brake torque of interest from which information on regions of stable and unstable braking can be easily extracted.

## 2.6. Hysteresis in the Single-Wheel Braking Model

The dimensionless function  $h_b(s)$  and the  $(u, s)$  dynamics reveal certain features of the system that may otherwise be difficult to extract. Referring again to Figure 5, consider the case when the saddle-node bifurcation has already occurred and that the current state of the system is that of wheel lockup (Fig. 5e). One may intuitively guess that the brake torque need only be reduced to a value slightly less than  $\Upsilon_b^{cr} = 15.250$  in order for stable braking to again be restored. This, however, is not the case. Although the stable invariant point  $s^+$  reappears, the state of the system remains at  $(u, 1)$ , or wheel lockup since that point remains stable as well. In fact,  $\Upsilon_b$  must be more drastically reduced below the value  $\Upsilon_b^L$  such that  $h_b(1) < 0$ , that is, lockup must be destabilized in order to restore stable braking conditions. Once this occurs, the system state jumps from wheel lockup to stable braking conditions. This ‘jump phenomenon’ may be conveniently captured by a bifurcation diagram.

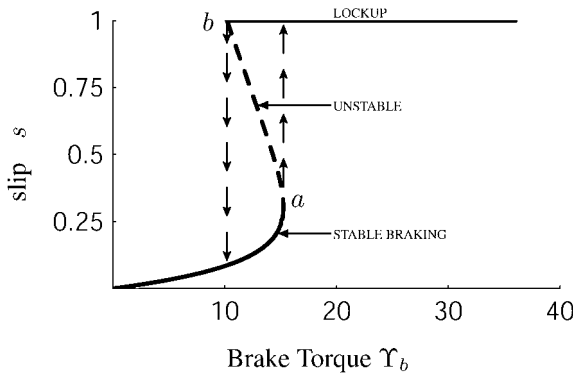


Fig. 6. Bifurcation diagram for the single-wheel braking model.

Figure 6 shows a plot of the invariant points  $s^*$  versus the brake torque. The upper- and lower-branch solid lines correspond to the stable steady-slip values  $s = 1$  (denoted by *lockup*) and  $s^+$  (denoted by *stable braking*), respectively, while the dashed line corresponds to the values  $s^-$  (denoted by *unstable*). The nonlinearity in  $s$  of the friction coefficient forms a region where the slip is multivalued. It is this multiplicity of steady-slip values that is responsible for the jump phenomenon and hysteresis behavior. As  $\Upsilon_b$  is increased from zero, the state of the system is governed by the stable lower branch. Eventually slip destabilizes at a value corresponding to point  $a$  (where  $\Upsilon_b = \Upsilon_b^{cr}$  and  $s = s_{cr}$ ) and jumps to the upper branch at wheel lockup. In order to restore stable braking conditions, the brake torque must be reduced to a value corresponding to the point  $b$  (where  $\Upsilon_b < \Upsilon_b^L$  such that  $h_b(1) < 0$ ) where lockup destabilizes causing slip to jump back to the stable lower branch.

### 2.7. The Transition to Unstable Braking

When a brake torque is applied to a rubber tire a tractive force is generated at the tire/road interface, as described in Section 2.1. The standard thinking is that the brake torque can increase until wheel slip reaches the value  $s_p$ , beyond which lockup occurs [1, 2]. Under steady-state braking conditions, the corresponding maximum brake torque is thus typically taken to be:

$$T_b^p = mgR\mu(s_p), \tag{21}$$

which is the maximum moment that can be provided by the friction force  $X = \mu(s_p)Z = \mu(s_p)mg$  about the wheel center. Thus, it is traditionally assumed that the critical brake torque at which the lockup instability is impending and the peak brake torque are the same, and that the transition to wheel lockup occurs

at  $s = s_p = s_{cr}$ . In what follows, it is shown that the lockup instability *does not occur at the peak value*  $s_p$  corresponding to the maximum of the  $\mu(s)$  curve, but at a condition that is typically nearby. It is subsequently shown that Equation (21) is actually only an approximation that is accurate when the vehicle to tire/wheel inertia ratio  $\nu$  is large.

### 2.7.1. Lockup Instability

Differentiating Equation (15) with respect to  $s$  and evaluating the resulting expression at critical slip yields:

$$h'_b(s_{cr}) = \mu'(s_{cr})(s_{cr} - 1 - \nu) + \mu(s_{cr}) = 0. \quad (22)$$

Recall that  $s_{cr}$  is the saddle node value in the slip dynamics, where, necessarily, the slope of  $h_b(s)$  is zero. Since in Equation (22),  $\mu(s_{cr}) > 0$  and  $(s_{cr} - 1 - \nu) < 0$ , it follows that:

$$\mu'(s_{cr}) = \frac{-\mu(s_{cr})}{s_{cr} - 1 - \nu} > 0. \quad (23)$$

Equation (23) shows that the slope of the friction characteristic  $\mu(s)$  at the critical value  $s = s_{cr}$  is positive, rather than zero, whereas  $\mu'(s_p) = 0$ . This means that, for wet or dry asphalt characteristics,  $s_{cr}$  is actually *smaller* than the peak value  $s_p$ . Hence, the lockup instability, or the transition to unstable braking, corresponds not to  $s_p$ , the peak of  $\mu(s)$ , but to the critical value  $s_{cr}$ , which is the minimum of  $h_b(s)$ .

These results are consistent with numerical evidence. Recall that the peak value  $\mu_p = \mu(s_p)$  of Equation (7) occurs at  $s_p = 0.316$ , whereas  $s_{cr} = 0.304$ , which is approximately 4% less than  $s_p$ . The corresponding critical brake torque is outlined next, from which Equation (21) can be obtained by invoking a series of approximations.

### 2.7.2. The Critical Brake Torque

Recall from Section 2.5 that the vehicle must come to rest under steady-slip conditions for which  $s = 1$  (wheel lockup) or  $s = s^*$ . The brake torque corresponding to a steady-slip value  $s = s^*$  follows from Equation (15) and is given by:

$$\Upsilon_b = -(s^* - 1 - \nu)\mu(s^*), \quad (24)$$

which is obtained by invoking the condition  $h_b(s^*) = 0$ . The critical brake torque  $\Upsilon_b^{cr}$  corresponding to steady-slip conditions is obtained by maximizing Equation (24) with respect to  $s$ . The result is:

$$\left. \frac{\partial \Upsilon_b}{\partial s} \right|_{s=s^*} = \mu'(s^*)(s^* - 1 - \nu) + \mu(s^*) = 0. \quad (25)$$

Equation (25) is of the same form as Equation (22), which is the expression that minimizes  $h_b(s)$ . Thus, it must be true that the critical brake torque is given by Equation (24) with the steady-slip value  $s^* = s_{cr}$  satisfying Equation (22). Recalling that  $\Upsilon_b = \frac{R}{Jg} T_b$  and  $\nu = \frac{mR^2}{J}$ , the critical brake torque can be written in the dimensional form:

$$T_b^{cr} = mgR\mu(s_{cr}) \left( 1 + \frac{1}{\nu}(1 - s_{cr}) \right). \quad (26)$$

Equation (26) indicates that the typically assumed maximum brake torque given by Equation (21) follows from two fundamental assumptions: (1) the inertia ratio  $\nu$  of the vehicle is large relative to unity; and (2) the peak slip value  $s_p$  can be attained. These assumptions are generally acceptable so that, for many applications, the true critical brake torque can be reasonably approximated by the assumed brake torque given by Equation (21). This is shown next.

Idealizing the wheel as a thin uniform disk of mass  $m_{wheel}$ , it follows that:

$$\nu = \frac{mR^2}{J} = 2 \frac{m}{m_{wheel}}, \quad (27)$$

where, recall,  $m$  is the mass of the vehicle/wheel combination. In most applications  $m \gg m_{wheel}$  so that  $\nu \gg 1$ . Moreover, the peak value  $s_p$  and  $s_{cr}$  are typically close. Referring again to Equation (7) and noting that  $\mu(s_{cr}) = \mu(0.304) = 0.972$ , it follows that  $\Upsilon_b^p = 14.574$  for  $\nu = 15$ . Numerical simulations show that  $\Upsilon_b^p = 15.250$  (see Fig. 5), rendering the approximation given by Equation (21) in error by less than 5%.

### 3. THE SINGLE-WHEEL ACCELERATION MODEL

This section describes a single-wheel vehicle acceleration model. Here, the term acceleration refers to the positive rate of change of velocity in the longitudinal direction due to an engine torque. Longitudinal acceleration is fundamentally dependent on two main limitations: engine power and traction [1]. However, the ensuing investigation assumes that sufficient engine power is available at any given instant to maintain a constant torque on the wheel. Thus, focus is shifted to understanding tractive properties, their dynamic characteristics, and how to maximize them.

The single-wheel vehicle acceleration model is physically identical to that of the single-wheel braking model, consisting of a tire/wheel disk with radius  $R$  and polar moment of inertia  $J$ . As depicted in Figure 7, it is constrained to move longitudinally in the  $x$ -direction with its speed denoted as  $u$ . The available engine torque, acting in the positive sense on the wheel, is denoted by  $T_e$ . The vertical reaction force  $Z$  balances the static weight  $mg$ , while the longitudinal force  $X$  serves to accelerate the vehicle.

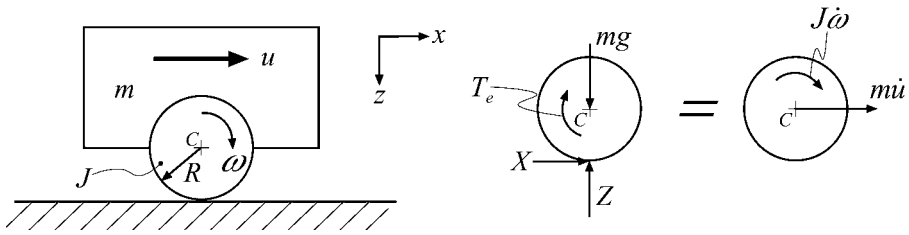


Fig. 7. Schematic of the single-wheel acceleration model and corresponding free body diagram.

The forward vehicle speed  $u$  and longitudinal wheel slip  $s$  are chosen as dynamic states. In vehicle acceleration it is assumed and taken as convention that  $\omega R > 0$  and  $0 \leq u \leq \omega R$ . Thus, wheel slip  $s = \frac{u - \omega R}{\max(u, \omega R)} = \frac{u - \omega R}{\omega R}$  is defined on the interval  $-1 = [-1, 0]$ , taking on the limiting values  $s = -1$  for pure slip ( $u = 0$ ) and  $s = 0$  for free rolling without slip ( $u = \omega R > 0$ ). The former case when  $u = 0$  indicates finite rotation of the wheel while maintaining zero vehicle speed. This is possible only in the presence of an externally applied force on the vehicle, which is not present in our model, to maintain  $u = 0$ . The case when  $u = \omega R$  implies the absence of an engine torque.

The Pacejka tire model could be employed in vehicle acceleration studies by letting  $s \rightarrow -s$  in the Magic Formula [Equation (6)]. For the present study of acceleration, we use the slip characteristic

$$\mu(s) = c_1(1 - e^{c_2 s}) + c_3 s, \tag{28}$$

with  $c_1 = 1.18$ ,  $c_2 = 10.0$ , and  $c_3 = 0.5$ , which is similar to Equation (7). As indicated in Figure 3, it is simply the reflection of  $\mu(s)$  used for braking about the vertical axis through  $s = 0$ , and thus has a peak value  $\mu_p = 0.972$  at  $s_p = -0.316$ .

### 3.1. Equations of Motion

Assuming that the friction law given by Equation (5) holds and making the appropriate substitutions, the equations of motion can be cast in the form:

$$\left. \begin{aligned} \dot{u} &= \mu(s)g \\ \dot{s} &= \frac{g}{u} h_a(s) \end{aligned} \right\}, \quad u > 0, \quad s \in (-1, 0]. \tag{29}$$

The nondimensional function  $h_a(s)$  is given by:

$$h_a(s) = (s + 1)^2 [(s + 1)^{-1} \mu(s) + \nu \mu(s) - \Upsilon_e], \tag{30}$$

where, again,  $\nu = \frac{mR^2}{J}$  is the vehicle/wheel inertia ratio and  $\Upsilon_e = \frac{R}{Jg} T_e$  is the dimensionless engine torque.

### 3.2. Steady-Slip Conditions and Local Stability

For nonzero  $u$  and a constant slip value  $s^*$  for which  $h_a(s^*) = 0$ , Equation (29) shows that wheel slip remains invariant, independent of the vehicle speed. Correspondingly, the forward vehicle acceleration is positive and constant, and its speed monotonically increases according to the equation:

$$u(t) = u_o + \mu(s^*)gt, \quad t \geq 0, \quad (31)$$

where  $u_o > 0$  is the initial speed when  $s = s^*$ , that is, when  $t = 0$ . Clearly the vehicle cannot continue to accelerate indefinitely. Due to aerodynamic drag, saturation of engine power, and so on, generation of the prescribed engine torque eventually becomes impossible. In order to quantify this limiting case one must include other factors in the dynamic model, which will not be considered here.

Local stability of the invariant points  $s^*$  follows in the same manner as discussed for the single-wheel braking model. (See Section 2.4). Stable and unstable fixed points are defined to be:

$$s^\pm = \{s | h_a(s^\pm) = 0, h'_a(s^\pm) \gtrless 0\},$$

and the corresponding invariant manifolds are given by:

$$\mathcal{W}_a^\pm = \{(u, s) | u > 0, s = s^\pm\}.$$

Note that the set  $\{(u, s) | u > 0, s = -1\}$  does not define an invariant manifold, since  $s$  is singular when  $u = 0$ .

### 3.3. Global Features of the Single-Wheel Vehicle Acceleration Model

The dynamic equations describing the single-wheel acceleration model are of the same structure as their braking model counterparts, with the only significant differences appearing in  $h_a(s)$ . Whereas the brake torque appears simply as an additive term in the function  $h_b(s)$  of the single-wheel braking model [Equation (15)], the engine torque is scaled by the nonlinear term  $(s + 1)^2$  in the function  $h_a(s)$  of the single-wheel acceleration model [Equation (30)]. It is this nonlinearity that yields slightly more complicated dynamics as the engine torque parameter  $\Upsilon_e$  is varied.

Depicted in Figure 8 is an example plot of the function  $h_a(s)$  versus slip and the corresponding state space dynamics in  $u$  and  $s$  for  $\nu = 15$  and  $\Upsilon_e = 15.65$ . At this parameter value there are two stable invariant points  $s^\pm$ , which define two invariant manifolds  $\mathcal{W}_a^+$ , and a single unstable steady-slip value  $s^-$  that defines the invariant manifold  $\mathcal{W}_a^-$ . As with the single-wheel braking model of Section 2, a single function  $h_a(s)$  describes completely the nonlinear dynamic behavior of the single-wheel acceleration model. The full range of dynamic possibilities is captured by the

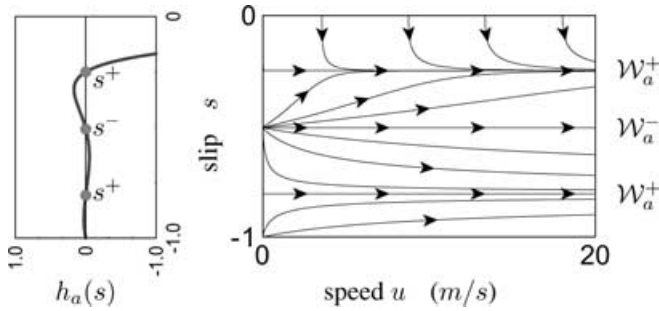


Fig. 8. Example plot of  $h_a(s)$  versus  $s$  and corresponding state space descriptions in  $u$  and  $s$  for  $\nu = 15$  and  $\Upsilon_e = 15.65$ .

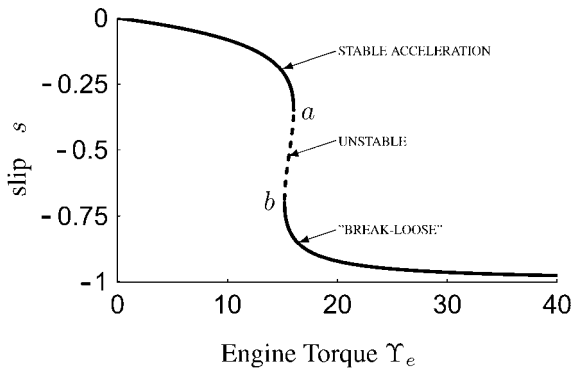


Fig. 9. Bifurcation diagram for the single-wheel acceleration model.

bifurcation diagram shown in Figure 9, which shows a plot of the invariant points  $s^*$  versus the engine torque. The upper- and lower-branch solid lines correspond to the stable steady-slip values  $s^+$  (denoted by *stable acceleration* and *break-loose*, respectively) while the dashed line corresponds to the values  $s^-$  (denoted unstable). As the engine torque is increased from zero, the state of the system is governed by the stable upper branch. Eventually slip destabilizes at value corresponding to point  $a$  and jumps to the lower branch, on which the slip is quite large, implying that there is significant wheel spin with relatively little forward acceleration. Physically, this corresponds to a very sudden increase in wheel spin, known in the colloquial as ‘burning out’ or ‘peeling out,’ and labeled as ‘break-loose.’ By further increasing the engine torque  $s$  approaches, but never reaches, pure slip at  $s = -1$ . In order to reestablish low-spin stable acceleration, the engine torque must be decreased to a level corresponding to point  $b$ , where slip jumps back to the stable upper branch.

#### 4. CONCLUSIONS AND DIRECTIONS FOR FUTURE WORK

The results presented here offer new insight into the behavior of vehicles during longitudinal braking and acceleration. In each case considered, the unique features of the modeling approach allow one to capture the full range of dynamic behavior of single-wheel models in a simple geometrical manner. By choosing the forward vehicle speed and longitudinal wheel slip as dynamic states, the dynamic equations of motion lend themselves to a relatively simple investigation and interpretation using the tools from nonlinear dynamics. This choice of dynamic states, where wheel slip plays a central role, allows the dynamics for the entire range of vehicle speeds and slip values to be captured by a single function (one each for braking and acceleration). These functions completely describe the tractive behavior of a given vehicle on a given road surface in terms of slip and the brake or engine torque. The relative simplicity of the analyses described herein is a consequence of the choice of dynamic states and the interpretation of the resulting equations of motion.

Perhaps the most important conclusion from this work is the fact that the lockup instability in the single-wheel model does not occur when the brake torque leads to the maximum point on the slip curve, but at a lower brake torque. The traditional assumption – that attaining the maximum coefficient of friction leads to lockup – is shown to be an approximation that is accurate only when the tire/wheel inertia is small compared to the vehicle inertia. Since this ratio is typically small, the approximation is quite good. However, when considering a light vehicle with relatively large tire/wheel inertia, the approximation becomes less accurate. In either case, it is of interest to note that the commonly held view of lockup for the single-wheel model is only an approximation.

This analysis is the first step in a new direction for the modeling of longitudinal ground vehicle traction, and much remains to be done. Two-wheel traction models are considered in a companion paper [7], although the two-wheel acceleration model has not been studied in detail. Some other lines of future work include more detailed parameter studies for specific vehicles under various road conditions, and the incorporation of these models into ABS/TCS development, where slip also plays a central role.

#### ACKNOWLEDGEMENTS

This work was supported in part by the Department of Applied Mechanics at the Budapest University of Technology and Economics, the Department of Mechanical Engineering & the Institute for Global Engineering Education at Michigan State University, the US-Hungarian Joint Fund for Technological Development, and by a grant from the National Science Foundation. The authors wish to thank Mr. Craig

Gunn of Michigan State University and Mr. Jim Schramski of ACRA, Incorporated for reviewing this manuscript. Thanks are also due to Professor Brian Feeny of Michigan State University for his insight and helpful comments.

## REFERENCES

1. Gillespie, T.: *Fundamentals of Vehicle Dynamics*. Warrendale, Society of Automotive Engineers (SAE), Inc, 1992.
2. Wong, J.: *Theory of Ground Vehicles*. Wiley, New York, 1978.
3. SAE Standard: Antilock Brake System Review. *SAE Paper* No. Iaa46, 1992, pp. 90–102.
4. Bakker, E., Nyborg, L. and Pacejka, H.: Tyre modelling for use in vehicle dynamics studies. *SAE Paper* No. 870421, 1987, pp. 190–204.
5. Bakker, E., Pacejka, H. and Lidner, L.: A new tire model with and application in vehicle dynamics studies, *SAE Paper* No. 890087, 1989, pp. 101–113.
6. Liu, Y. and Sun, J.: Target slip tracking using gain-scheduling for antilock braking systems. *Proceedings of the American Control Conference*, 2 (June 1995), pp. 1178–1182.
7. Olson, B., Shaw, S. and Stépán, G.: *Stability and bifurcation of longitudinal vehicle braking*. Preprint, Department of Mechanical Engineering, Michigan State University, USA.
8. Kobayashi, K., Cheok, K.C. and Watanabe, K.: Estimation of absolute vehicle speed using fuzzy logic rule-based kalman filter. *Proceedings of the American Control Conference* 5 (1995), pp. 3086–3090.
9. Goodenow, G., Kolhoff, T. and Smithson, F.: Tire-road friction measuring system – a second generation. *SAE Paper* No. 680137, 1968, pp. 571–579.
10. Harned, J., Johnston, L. and Scharpf, G.: Measurement of tire brake force characteristics as related to wheel slip (antilock) control system design. *SAE Paper* No. 690214, 1969, pp. 909–925.
11. Sitchin, A.: Acquisition of transient tire force and moment data for dynamic vehicle handling simulations. *SAE Paper* No. 831790, 1983, pp. 1098–1110.